A Theoretical and Experimental Study on Acid-Catalyzed Isomerization of 1-Acylaziridines to the Oxazolines. Reexamination of a Possible S_Ni Mechanism by Using *ab Initio* Molecular Orbital Calculations

Kenzi Hori,*[,1a] Takeshi Nishiguchi,[1b] and Aiko Nabeya[1c]

Institute for Fundamental Research of Organic Chemistry, Kyushu University, Fukuoka 812-81, Japan, Faculty of Education, Yamaguchi University, Yamaguchi 753, Japan, and Department of Chemistry, Turumi University, School of Dental Medicine, Yokohama 230, Japan

Received June 10, 1996 (Revised Manuscript Received February 5, 1997[⊗]*)*

The S_Ni mechanism, which was previously proposed for the isomerization of 1-acylaziridines to the oxazolines, was reexamined theoretically by performing molecular orbital (MO) calculations of 1-formylaziridine and its derivatives as model compounds and experimentally by using 1(*R*)-[α-methoxy-α-(trifluoromethyl)phenylacetyl]-2(*S*)-methylaziridine (**5**). At the MP2/6-31G**//RHF/6-31G* level, the activation energy was estimated to be 38.9 kcal mol^{-1} for the S_Ni mechanism in which N-protonated 1-formylaziridine **8a**(NH^+) isomerizes to the N-protonated oxazoline **9a**(NH^+). Intrinsic reaction coordinate calculations showed that this reaction proceeds with retention of the ring carbon configuration. Methyl substitution in the aziridine ring reduces the activation energy by 10 kcal mol^{-1}. The ring closure of N-(2-chloroethyl)formamide (**10a**) to the oxazoline, which is a model reaction of the rate-determining step for the addition−elimination mechanism, was estimated to have an activation energy of 45.4 kcal mol^{-1}. The results of these MO calculations are consistent with the observation that the isomerization of the acylaziridine **5** to the oxazoline **6** is facilitated in the presence of weak nucleophiles such as with $BF_3{\cdot}OEt_2$ while the formation of **6** is very slow in the presence of stronger nucleophiles such as *p*-toluenesulfonate. Both theoretical and experimental results suggest that the S_Ni mechanism explains well the isomerization of (*R*,*S*)-**5** to the oxazoline with $BF_3{\cdot}OEt_2$ in refluxing benzene.

Introduction

Convincing experimental evidence for the S_Ni mechanism only exists for a relatively few reactions.[2,3] Two of the most important examples are the decomposition of alkyl chlorosulfites (ROSOCl) and chloroformates (ROCOCl) to the alkyl chlorides. For these reactions, four-centered cyclic transition states, leading to front-side substitutions and resulting in the retention of the configuration, have been proposed.[4] However, the existence of such transition states has been challenged. An "ion pair, multi-stage substitution" has been advanced to explain the acceleration of the reactions in polar solvents and the change of products depending on the reaction conditions.[5] Recently, Schreiner et al. elucidated the decomposition of ROSOCl using both theoretical and experimental methods.[6] They termed the decomposition with R = *tert*-butyl and 1-adamantyl the S_N1i mechanism (i.e., the S_N1-like S_Ni) mechanism.

We earlier reported another reaction which possibly proceeds by the S_Ni mechanism (eq 1).[7a] More specifically, (S)-1-(*N*-phenylcarbamoyl)-2-methylaziridine (**1**) isomerizes into (*S*)-2-anilino-5-methyl-2-oxazoline (**2**) with complete retention of configuration at the asymmetric carbon when it was heated in refluxing benzene with $BF_3{\cdot}OEt_2$. In this reaction, 4-methyl isomer was also observed and the ratio of 5-methyl/4-methyl products was 88/12. Similarly a benzene solution of boron trifluoride free of diethyl ether was found to smoothly isomerize the aziridine derivatives to the oxazolines. This reaction also preserved the carbon configuration in the five-membered ring of the product completely (eq 2): *cis*-1-

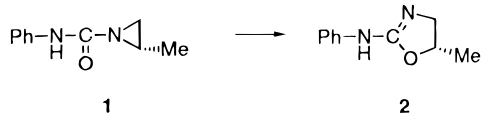

(1)

1 **2**

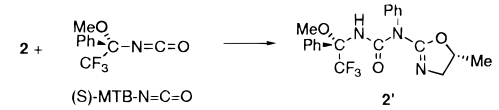

2'

⊗ Abstract published in *Advance ACS Abstracts,* April 1, 1997.

(1) (a) Kyushu University. (b) Yamaguchi University. (c) Tsurumi University.

(2) Gould, E. S. *Mechanism and Structure in Organic Chemistry*; Henry Holt and Company Inc.: New York, 1960; p 294.

(3) March, J. *Advanced Organic Chemistry: Reactions, Mechanisms, and Structure*; 4th ed.; Wiley-Interscience: New York, 1992; pp 308, 326.

(4) (a) Cowdrey, W. A.; Hughes, E. D.; Ingold, C. K.; Masterman, S.; Scott, A. D. *J. Chem. Soc.* **1937**, 1252. (b) Hughes, E. D.; Ingold, C. K.; Whitfield, I. C. *Nature* **1941**, *147*, 206. (b) White, E. H. *J. Am. Chem. Soc.* **1954**, *76*, 4497. (b) White, E. H.; Aufdermarsh, Jr. *J. Am. Chem. Soc.* **1961**, *83*, 1179. (c) Lewis, E. S.; Herndon, W. C.; Duffy, D. C. *J. Am. Chem. Soc.* **1961**, *83*, 1959. (d) Stevens, C. L.; Munk, M. E.; Ash, A. B.; Elliott, R. D. *J. Am. Chem. Soc.* **1963**, *85*, 3390. (e) Stevens, C. L.; Dittmer, H.; Kovacs, J. *J. Am. Chem. Soc.* **1963**, *85*, 3394. (f) Christe, K. O.; Pavlath, A. E. *J.* Org. *Chem.* **1965**, *30*, 4104.

(5) (a) Cram, D. J. *J. Am. Chem. Soc.*, **1953**, *75*, 332. (b) Lewis, E. S.; Boozer, C. E. *J. Am. Chem. Soc.* **1952**, *74*, 308. (c) Boozer, C. E.; Lewis, E. S. *J. Am. Chem. Soc.* **1953**, *75*, 3182. (d) Lewis, E. S.; Coppinger, C. E. *J. Am. Chem. Soc.* **1954**, *76*, 796. (e) Lee, C. C.; Finlayson, A. J. *Can. J. Chem.* **1961**, *39*, 260. (f) Lee, C. C.; Clayton, J. W.; Lee, D. G.; Finlayson, A. J. *Tetrahedron* **1962**, *18*, 1395. (g) Lee, C. C.; Newman, D.; Thornhill, D. P. *Can. J. Chem.*, **1963**, *41*, 620. (h) White, E, H.; Ellinger, C. A. *J. Am. Chem. Soc.*, **1965**, *87*, 5261.

(6) (a) Schreiner, P. R.; Schleyer, P. R.; Hill, R. K. *J. Org. Chem.* **1993**, *58*, 2822, and references cited therein. (b) Schreiner, P. R.; Schleyer, P. R.; Hill, R. K. *J. Org. Chem.* **1994**, *59*, 1849.

(7) (a) Nishiguchi, T.; Tochio, H.; Nabeya, A.; Iwakura, Y. *J. Am. Chem. Soc.* **1969**, *91*, 5841. (b) Nishiguchi, T.; Tochio, H.; Nabeya, A.; Iwakura, Y. *J. Am. Chem. Soc.* **1969**, *91*, 5835. (c) We repeated the experiment with **1**, and ^{19}F NMR spectroscopy of the derivative of **2** (**2'**) confirmed the 100% retention of the configuration more precisely. See Nabeya, A.; Endo, T. *J. Org. Chem.* **1988**, *53*, 3358.

S0022-3263(96)01089-4 CCC: $14.00

Scheme 1

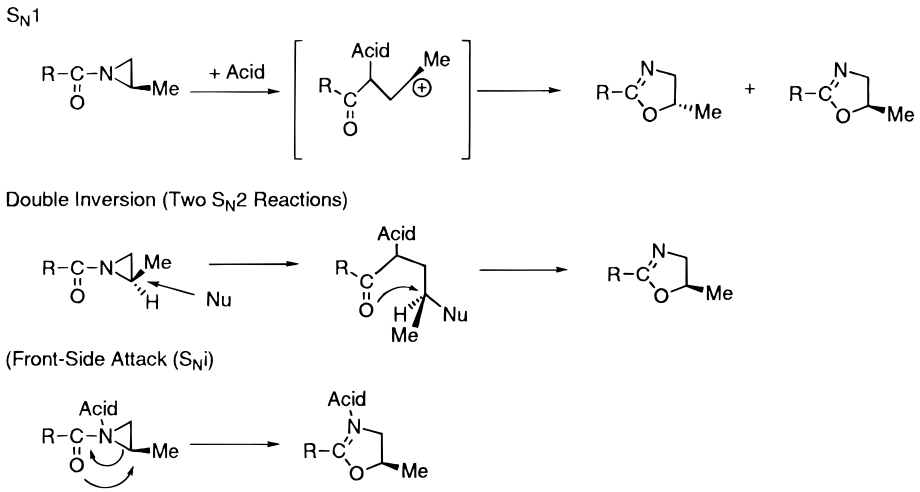

(*N*-phenylcarbamoyl)-2,3-dimethylaziridine (**3**) gave *cis*-2-anilino-4,5-dimethyl-2-oxazoline (**4**) when it was heated in refluxing benzene with BF_3.[7c]

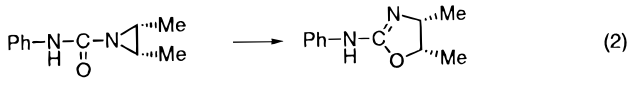

(2)

3 **4**

In order to examine the mechanism of these reactions, we performed *ab initio* molecular oribital (MO) calculations of 1-formylaziridine and its derivatives as model molecules. In this connection, we examined the reaction mechanism of 1(*R*)-[α-methoxy-α-(trifluoromethyl)phenylacetyl]-2(*S*)-methylaziridine (**5**). All the molecules are aziridines with an amide fragment. It was experimentally confirmed that the reaction of **5** with BF_3·OEt_2 only produced the oxazoline **6** while the reaction of **5** with *p*-toluenesulfonic acid (TsOH) mainly gave a linear product **7** together with a small amount of **6**.

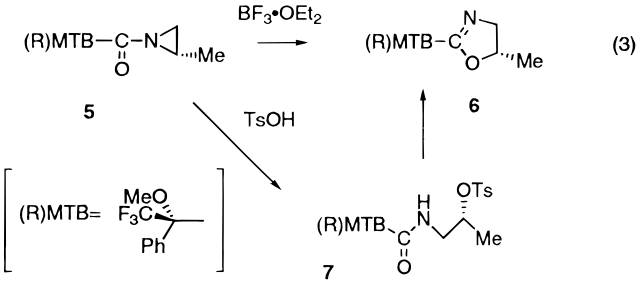

(3)

5 **6** **7**

There are three feasible mechanisms for the reactions we observed.[8] The first, shown in Scheme 1, is an S$_N$1 mechanism via a carbenium ion intermediate. However, this mechanism would cause racemization and produce a mixture of the products with *S*- and *R*-configurations in the five-membered ring. Therefore, the S$_N$1 mechanism cannot explain our experimental results. The second, the double inversion mechanism, is an addition−elimination mechanism which involves two S$_N$2 type reactions. The tosylate nucleophile attacks the aziridine ring to form the open chain intermediate **7** followed by attack of amide oxygen atom to displace the tosylate. These two Walden inversions proceed with a net retention of the ring carbon configuration. The last is a front side attack of the carbonyl oxygen directly on the ring carbon to break the C−N bond (i.e., the S$_N$i mechanism) where the configuration of the ring carbon is retained in the products because the oxygen approaches from the same side as the leaving group (nitrogen) leaves.

In the present study, we performed *ab initio* MO calculations on the isomerization processes to examine the validity of the S$_N$i mechanism proposed before.[7] We examined in detail the acid-catalyzed isomerization of **8a**(NH^+) to the oxazoline **9a**(NH^+) using H^+ as a model acid. Chloride anion Cl^- was adopted as a model nucleophile instead of TsO^- for the double inversion mechanism which involves a reaction via a linear intermediate **10a**. In order to investigate the substituent effect, the reaction of **8b** with a methyl group was also investigated, and the changes in activation energies were estimated.

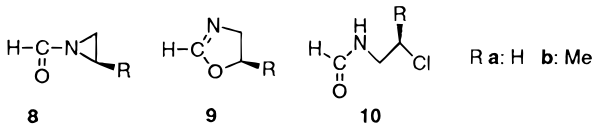

8 **9** **10**

Method of Calculations

The *ab initio* MO calculations were carried out using the GAUSSIAN92 program[9] running on a NEC-HSP computer at the Institute for Molecular Science and on the IBM RS6000 computer. MOPAC Ver. 6[10] was also used for the preliminary search of potential profiles of the reaction mechanisms considered here. Grand and transition state (TS) geometries were optimized by the

(8) It may be possible to consider another path that the reaction proceeds via a tight ion-pair intermediate of **8a**(NH^+) with the broken three-membered ring. Although we tried to optimize this intermediate by using several initial geometries, we failed to optimize it and obtained the product with a five-membered ring. This result suggests that the there is no tight ion-pair intermediate with a broken three-membered ring.

(9) Gaussian 92, Revision D.2, M. J. Frish, G. W. Trucks, M. Head-Gordon, P. M. W. Gill, M. W. Wong, J. B. Foresman, B. G. Johnson, H. B. Schlegel, M. A. Robb, E. S. Replogle, R. Gomperts, J. L. Andres, K. Raghavachari, J. S. Binkley, C. Gonzalez, R. L. Martin, D. J. Fox, D. J. Defrees, J. Baker, J. J. P. Stewart, J. A. Pople, Gaussian, Inc., Pittsburgh PA, 1992.

(10) (a) MOPAC Ver.6., Stewart, J. J. P. *QCPE Bull.* **1989**, *9*, 10. (b) We performed semiempirical PM3 calculations, and then the obtained PM3 geometries were used as the initial geometries of the *ab initio* calculations. Although the PM3 geometries were not far from the 6-31G* geometries, the semiempirical calculation did not represent well the energy relation among reactants, intermediates, products, and TS.

(11) Hehre, W. J.; Ditchfield, R.; Pople, J. A. *J. Chem. Phys.* **1972**, *56*, 2257.

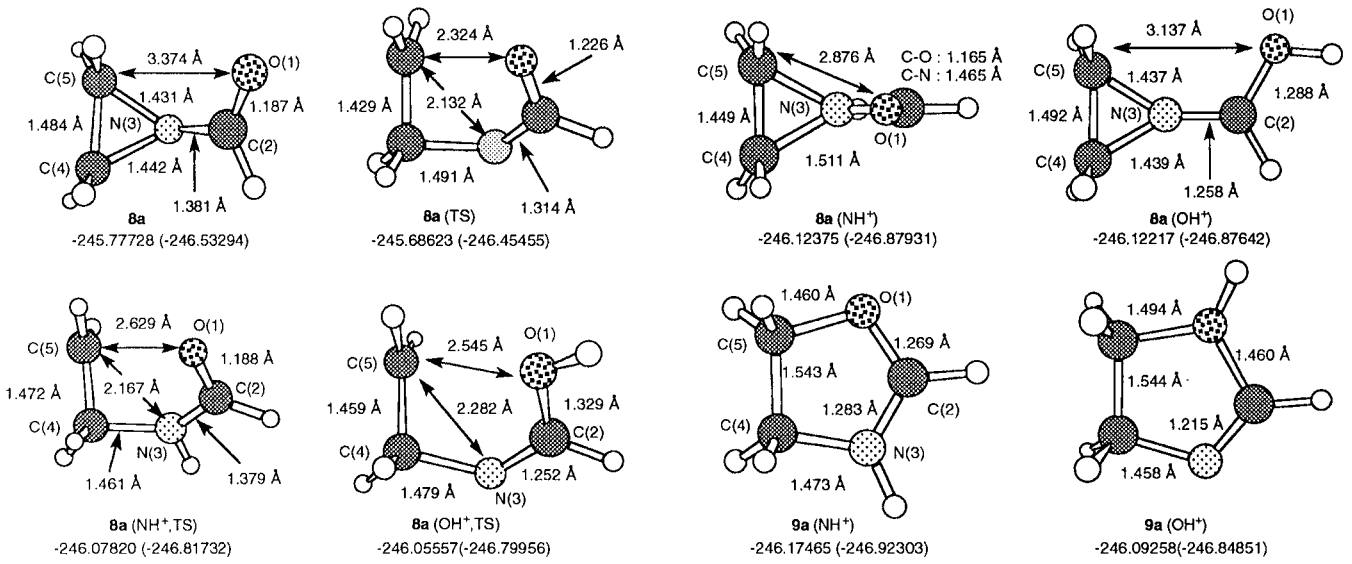

Figure 1. Optimized structures related to the S_Ni mechanism together with their geometrical parameters. Values under the molecules are the total energies in Hartree units calculated at the RHF/6-31G* (MP2/6-31G**//RHF/6-31G*) level of theory.

energy gradient method at the RHF/6-31G*[11] level of theory. The vibration frequency calculations showed that all the TS structures have only one imaginary frequency. The optimized structures of the proposed mechanisms and total energies are shown in Figure 1.

The intrinsic reaction coordinate[12] (IRC) method was used in order to obtain energy profiles of the reaction pathway via **8a**(TS), **8a**(NH^+,TS), **8a**(OH^+,TS), **8a**(Cl^-,TS) and **10a**(TS). The first three TS's relate to the S_Ni mechanism and the last two to the double inversion mechanism. We adopted 0.02 amu$^{1/2}$ Bohr as the step size for the IRC calculations. In order to study the effect of correlation, MP2/6-31G**//RHF/6-31G* energies were also calculated. Unless otherwise noted, all energies mentioned in the discussion are at this high level of theory.

Results and Discussions

Experimental Results. Amide (*R*,*S*)-**5** was prepared from (*S*)-2-methylaziridine and (*S*)-α-methoxy-α-(trifluoromethyl)phenylacetyl chloride (MTPA chloride). A solution of **5** dissolved in benzene was added to a refluxing solution of $BF_3{\cdot}OEt_2$ (1.1 mol equiv), and the reaction was monitored by TLC. After 15 min, the reaction was judged complete, and the solution was cooled, washed with 2 N NaOH and brine, dried (Na_2SO_4), and concentrated to give **6** in nearly quantitative yield. The ratio between (*R*,*S*)-**6** (^{19}F NMR: δ 3.18) and (*R*,*R*)-**6** (^{19}F NMR: δ 3.21) was found to be 97:3.

Reaction of (*R*,*S*)-**5** with TsOH was carried out in exactly the same way as mentioned above. After 15 min, a part of the reaction mixture was removed for NMR analysis. The ^{19}F NMR spectrum showed that the sample consisted of 92% of the ring-opened addition product, (*R*,*R*)-**7** and 8 % of (*R*,*S*)-**6**. After 1 h of heating, the composition of the reaction mixture was found to be the same as before.

The S_Ni Mechanism. In the acid-catalyzed isomerization of 1-acylaziridines, the first step is the coordination of an acid to either the ring nitrogen or the carbonyl oxygen of the substrate. In the present calculations, we used H^+ as the model acid instead of BF_3. Figure 1 displays the optimized structures of 1-formylaziridine **8a** and its N- and O-protonated forms, **8a**(NH^+) and **8a**(OH^+). The optimized C(4)−C(5) and N(3)−C(4),C(5) lengths in **8a** (1.484, 1.442, and 1.431 Å, respectively) are close to the corresponding lengths observed in aziridine.[13] The CHO plane of the acyl group is neither perpendicular nor periplanar to the NC_2 plane of the aziridine ring so that this geometrical feature results in the rather long O(1)−C(5) length of 3.374 Å.

Although the O-protonation to **8a** causes changes in bond lengths, the differences between the unprotonated and the protonated form are not very large in the three-membered ring. For example, in **8a**(OH^+) the O(1)−C(2) (1.288 Å) lengthens by 0.101 Å and the C(2)−N(3) bond (1.258 Å) shortens by 0.123 Å in comparison with those in **8a** (1.187 and 1.381 Å) while the bond lengths in the ring do not change at all (less than 0.01 Å). The CHO plane is periplanar to the NC_2 plane in the O-protonated form, and then, the O(1)−C(5) length is 3.137 Å which is shorter by 0.237 Å than that in **8a**.

The N-protonation causes two changes related to the ring geometry in **8a**(NH^+). The first is lengthening of the N(3)−C(4) and N(3)−C(5) bonds by ca. 0.07 Å (i.e., the protonation weakens these bonds). The second involves the angle between the CHO and the NC_2 planes. The CHO plane is almost perpendicular to the NC_2 plane so that the O(1)−C(5) length is shorter by 0.498 Å compared to that observed in the starting material **8a**. This length is also shorter by 0.216 Å than that in **8a**(OH^+). This short O(1)−C(5) distance should facilitate attack of the carbonyl oxygen at the C(5) position. The calculations of the protonated 1-formylaziridines in the MP2/6-31G**//RHF/6-31G* level of theory demonstrate that **8a**(NH^+) is more stable by 1.8 kcal mol^{-1} than **8a**(OH^+). Therefore, we first searched the TS structure **8a**(NH^+,TS) which connects **8a**(NH^+) and the N-protonated oxazoline **9a**(NH^+).

The IRC calculation demonstrates that **8a**(NH^+,TS) connects the reactant and the product as shown in Figure

(12) (a) Fukui, K. *Acc. Chem. Res.* **1981**, *14*, 363. (b) Head-Gordon, M.; Pople, J. A. *J. Chem. Phys.* **1988**, *89*, 5777.

(13) *Kagaku Binran*, Kiso-hen II, 3rd ed., Maruzen: Tokyo 1984; p 653.

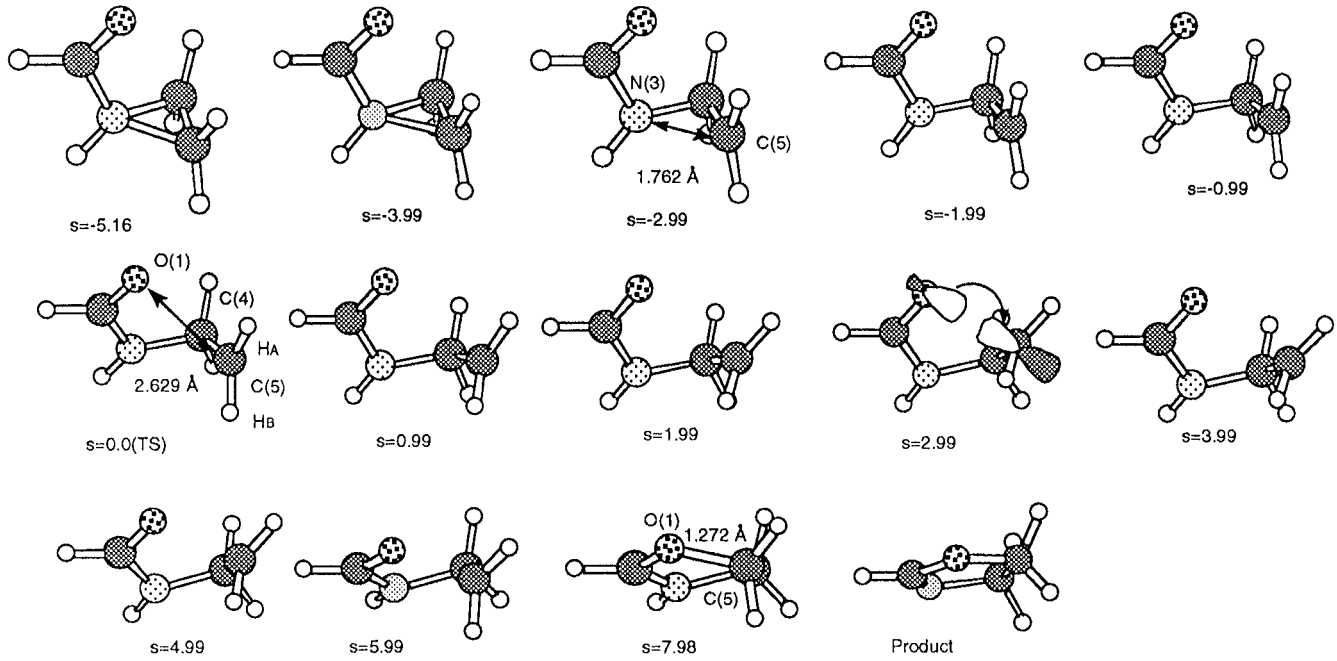

Figure 2. Geometry transformation along the IRC from **8a**(NH^+) to **9a**(NH^+) by the S_Ni mechanism. Values under the structures are the distances from the TS in $amu^{1/2}$ Bohr unit.[14]

2. The geometry at $s = -5.16$ $amu^{1/2}$ Bohr[14] is close to that of the reactant **8a**(NH^+) and the structure at $s = 7.98$ $amu^{1/2}$ Bohr resembles the product **9a**(NH^+). At $s = -2.99$ $amu^{1/2}$ Bohr, the N(3)−C(5) bond is essentially broken since the distance is 1.762 Å. The O(1)−C(5) length is 2.629 Å in the TS structure ($s = 0.0$ $amu^{1/2}$ Bohr). After the TS, the terminal $C(5)H_2$ plane is tilted in the geometries with $s = 0.99-5.99$ $amu^{1/2}$ Bohr. Such geometrical change allows better overlap of the empty p-orbital of the CH_2 moiety and the lone pair orbital at the carbonyl oxygen O(1) as shown in the geometry at $s = 2.99$ $amu^{1/2}$ Bohr. The O(1)−C(5) bond is fully developed at $s = 7.98$ $amu^{1/2}$ Bohr, and its length is 1.272 Å.

It is necessary to check whether or not the geometrical transformation along the IRC produces a change of the chirality around the ring carbon C(5). At the TS, the terminal carbon possesses almost sp^2 hybridization since the deihedral angle $\angle H_A-C(4)-C(5)-H_B$, is estimated to be −173.7°. The terminal CH_2 plane tilts a little after the TS in order to form a new O(1)−C(5) bond. However, around the C(4)−C(5) axis we cannot see the rotation which leads to the chirality change at C(5) in Figure 2.

The O(1)−C(5) and the N(3)−C(5) distances are good reaction coordinates for following the S_Ni mechanism. Figure 3 displays the distances along the IRC together with the potential energy profile. From $s = -6.0$ to −4.0 $amu^{1/2}$ Bohr, neither the N(3)−C(5) length (ca. 1.5 Å) nor the potential energy changes although the O(1)−C(5) length shortens by ca. 0.2 Å. Between $s = -3.99$ and 0.00 $amu^{1/2}$ Bohr, the O(1)−C(5) distance remains almost constant at 2.7 Å while the N(3)−C(5) distance lengthens by ca. 0.8 Å. The change in the potential energy almost parallels that of the length of the N(3)−C(5) bond. After the TS, the O(1)−C(5) distance shortens quickly to form the five-membered ring. The quick descent of the potential energy after the TS originates from this bond formation. On the other hand, the N(3)−C(5) distance fluctuates a little during this period.

(14) "*s*" in $amu^{1/2}$ Bohr units is a measure of the distance of a molecular configuration from the TS. See ref 12a.

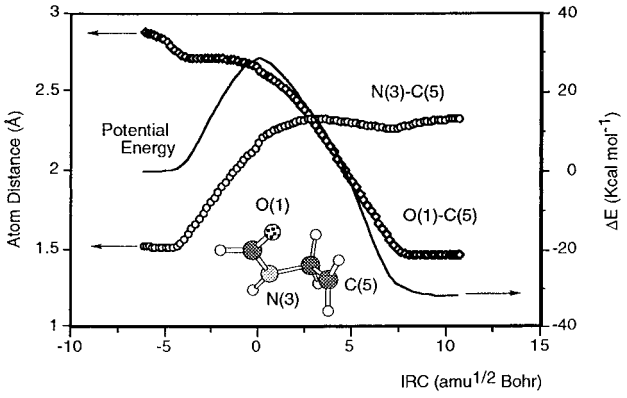

Figure 3. Potential energy profile (right) and the changes in the O(1)−C(5), (N3)−C(5) distances (left) along the IRC using RHF/6-31G* calculations.

In the isomerization from **8a**(NH^+) to **9a**(NH^+), from $s = -5.16$ $amu^{1/2}$ Bohr to the TS, the S_N1 type N(3)−C(5) bond cleavage occurs to form an "ion-pair" TS. From the TS to the product, the carbonyl oxygen attacks the C(5) center from the same side of the broken N(3)−C(5) bond as seen in Figure 2. Adopting the nomenclature proposed by Schreiner et al., we may describe the process as the S_N1i reaction.

The activation energy (E_a) of the N-protonated S_Ni mechanism is calculated to be 38.9 kcal mol^{-1} at the MP2/6-31G**//RHF/6-31G* level of theory. Figure 4 displays the energy diagram of the molecules under consideration. On the other hand, the E_a without protonation was calculated to be 49.2 kcal mol^{-1}, and therefore, addition of a simple Lewis acid reduces the activation barrier by 10.3 kcal mol^{-1}.

It is possible to consider an alternative mechanism that the O-protonated reactant **8a**(OH^+) isomerizes to the O-protonated product **9**(OH^+) via **8a**(OH^+,TS), whose structures are also displayed in Figure 1. The O(1)−C(5) length in **9a**(OH^+,TS) is shorter by 0.084 Å, and the N(3)−C(5) one is longer by 0.061 Å than the correspond-

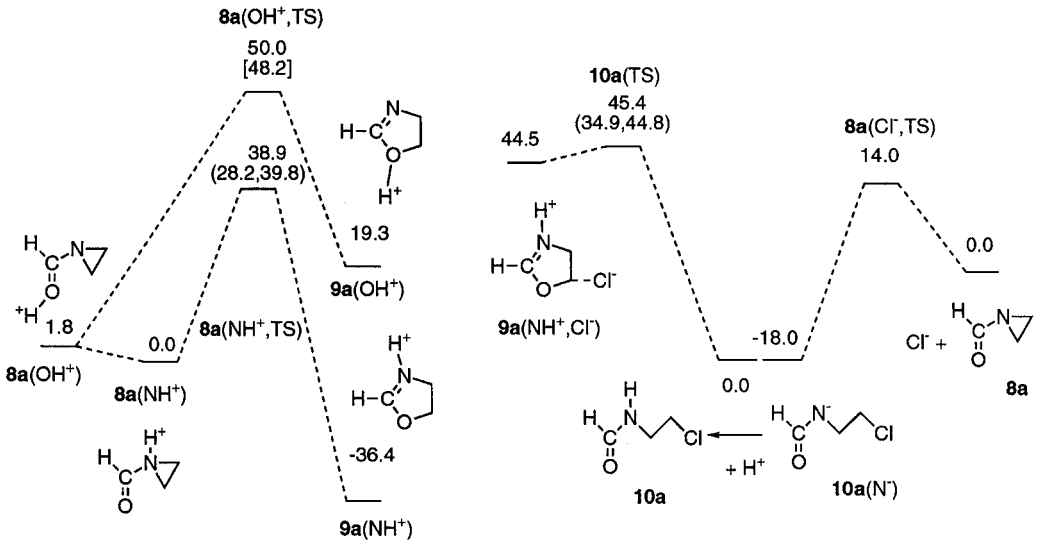

Figure 4. The energy relation diagram in kcal mol^{-1} unit among the reactants, the transition states, and the products. The values are relative to the total energy of **8a**(NH$^+$) or **8a**+Cl$^-$ or **10a**. Values in brackets and parentheses are the activation energies for the reaction from **8a**(OH$^+$) to **9a**(NH$^+$) and for the mechanism producing 5-methyl and 4-methyl derivatives of **9b**(NH$^+$), respectively.

ing lengths in **8a**(NH$^+$,TS). The E_a of the O-protonated path is 48.2 kcal mol^{-1}. The protonation at the carbonyl oxygen reduces the nucleophilicity of O(1) and **8a**(OH$^+$) is less stable by 1.8 kcal mol^{-1} than **8a**(NH$^+$). Therefore, the activation barrier in the O-protonated mechanism is larger by 11.1 kcal mol^{-1} than that in the N-protonated mechanism. Therefore, it is likely that the S_Ni reaction proceeds not via **8a**(OH$^+$,TS) but rather via **8a**(NH$^+$,TS).

Double Inversion Mechanism. Double inversion mechanism consists of two S_N2 reactions. The first involves the ring opening caused by the attack of a nucleophile on C(5) from the opposite side of the N(3) to form an acyclic intermediate. We used chloride as a model nucleophile in the present study. The MP2/6-31G**//RHF/6-31G* energies of **8a**+Cl$^-$ and **8a**(Cl$^-$,TS) are calculated to be −706.18175 and −706.20408 Hartree, respectively.[15] As the activation barrier is estimated to be only 14.0 kcal mol^{-1}, the ring opening caused by chloride attack appears very facile. This reaction accompanies the so-called Walden inversion seen in Figure 5 which displays the geometry transformation along the IRC. Starting at $s = -5.98$, the chloride nucleophile approaches the ring methylene moiety, and then, the N(3)−C(5) bond breaks at $s = -1.00$ amu$^{1/2}$ Bohr. The structure at $s = 7.01$ amu$^{1/2}$ Bohr, where a linear anionic intermediate has fully formed, has two H atoms directing to the another side of Cl$^-$. We do not see such a configuration change at the C(5) in the S_Ni mechanism mentioned above. After the formation of the anionic intermediate, it accepts an H$^+$ to form **10a**. It is important to point out that no TS structure for the ring opening was obtained for **8a**(NH$^+$) and **8a**(OH$^+$). It is, therefore, gathered that this reaction proceeds without protonation to the reactant.

The carbonyl oxygen O(1) functions as a nucleophile in the second S_N2 reaction. This reaction begins by attack of the carbonyl oxygen onto the C(5) center from the opposite direction of the Cl atom and ends with the formation of a five-membered ring. In Figure 6, we can see another Walden inversion around C(5). At $s = -5.85$ amu$^{1/2}$ Bohr, O(1), C(5), and Cl make nearly a straight alignment, which facilitates attack of O(1) on the C(5)-H_2Cl fragment. The C(5)−Cl bond disappears at $s = -2.99$ amu$^{1/2}$ Bohr since the length is 2.038 Å. At $s = -0.99$ amu$^{1/2}$ Bohr, the C(5) takes sp^2 hybridization because C(4) is almost in the plane defined by the C(5)-H_2 moiety. The five-membered ring has already formed (O(1)−C(5): 1.512 Å) and the C(5)−Cl length is 2.886 Å at $s = 2.54$ amu$^{1/2}$ Bohr so that the reaction has nearly completed at this point on the IRC pathway.

The MP2/6-31G**//RHF/6-31G* energies for the second S_N2 reaction are −706.79937, −706.72697, and −706.72701 Hartree for **10a**, **10a**(TS), and **9a**(NH$^+$,Cl$^-$), respectively. The activation barrier of this process is 45.4 kcal mol^{-1}.[16] The energy of the ring formation is higher by 24.9 kcal mol^{-1} than that of the first S_N2 reaction and by 6.5 kcal mol^{-1} than that of the S_Ni mechanism.

Substituent Effect. According to our experimental results, heating **5** in benzene with BF_3·OEt_2 produced exclusively the 5-methyloxazoline **6**, and no 4-methyl isomer is formed. In order to explain this behavior, we optimized the methyl-substituted aziridine **8b**(NH$^+$) and the two TS's, **8b**(5,NH$^+$,TS) and **8b**(4,NH$^+$,TS), leading to the formation of the 5-methyl- and 4-methyloxazolines, respectively. Figure 7 displays their optimized structures. As the N(3)−C(5) length (1.535 Å) is longer by 0.026 Å than the N(3)−C(4) one (1.509 Å) in **8b**(NH$^+$), the introduction of a methyl group on C(5) weakens the N(3)−C(5) bond.

The O(1)−C(5) length in **8b**(5,NH$^+$,TS) is 2.788 Å and the O(1)−C(4) distance in **8b**(4,NH$^+$,TS) is 2.607 Å. On the other hand, the three-membered ring is broken more

(15) Because the **8a**(TS,Cl$^-$) is an anion, we checked the effect diffuse functions for the activation energy. MP2/6-31+G**//RHF/6-31G* energies of Cl$^-$, **8a**, and **8a**(TS,Cl$^-$) are −459.67115, −246.54842, and −706.21702 Hartree, respectively. The activation energy is estimated to be 19.2 kcal mol^{-1} which is larger by 5.2 kcal mol^{-1} than the value from the calculation without diffuse functions. This value is still much smaller than that for the second S_N2 mechanism and for the S_Ni mechanism. The addition of diffuse functions does not cause any differences in the rank ordering of relative energies.

(16) The MP2/6-3+G**//RHF/6-31G* energies for the second S_N2 reaction are −706.81763, −706.74550, and −706.74669 Hartree for **10a**, **10a**(TS), and **9a**(NH$^+$,Cl$^-$), respectively. The activation energy for the second reaction is 45.3 kcal mol^{-1}, and the energy difference between the last two geometries is only 0.8 kcal mol^{-1}. The diffuse functions do not cause any serious differences, either.

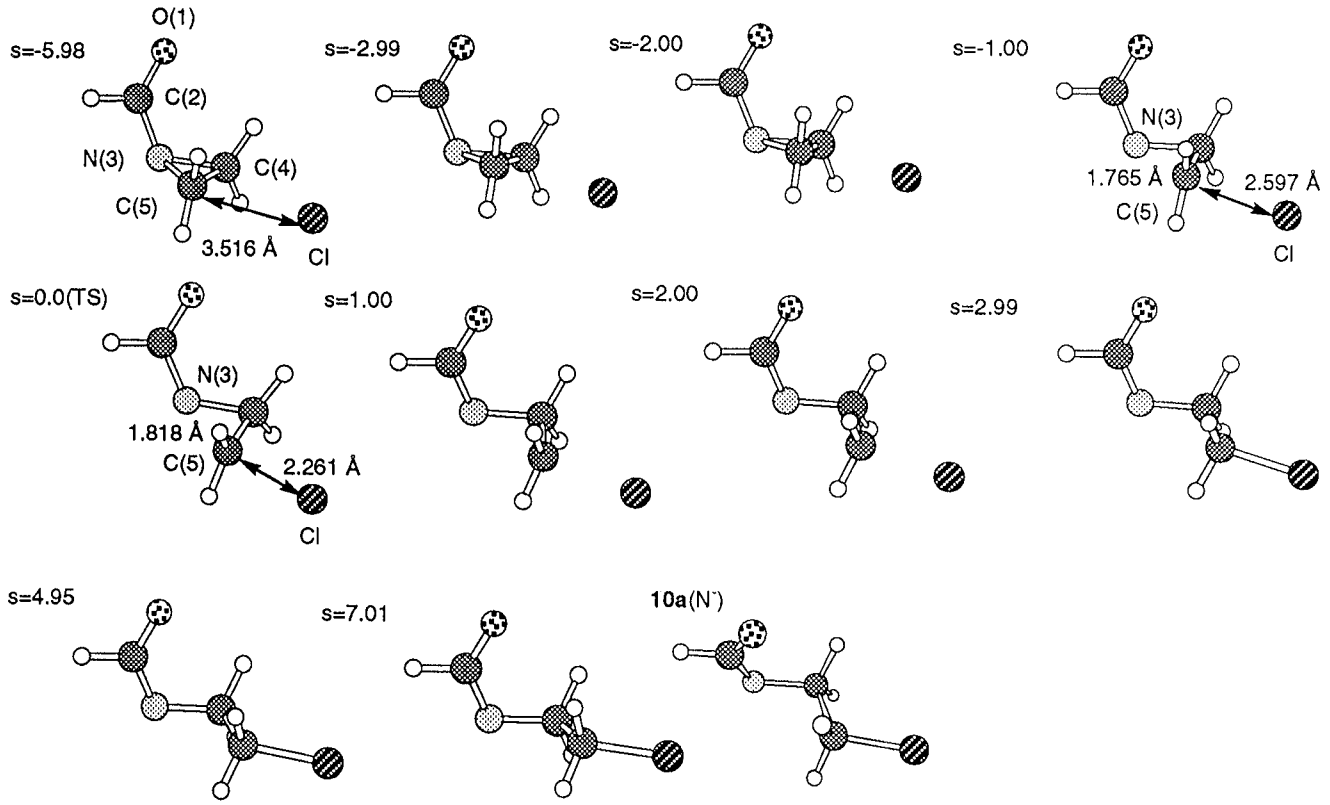

Figure 5. Geometry transformation along the IRC of the first S_N2 reaction from **8a**+Cl^- to **10a**(N^-). Values under the structures are the distances from the TS in $amu^{1/2}$ Bohr unit.[12]

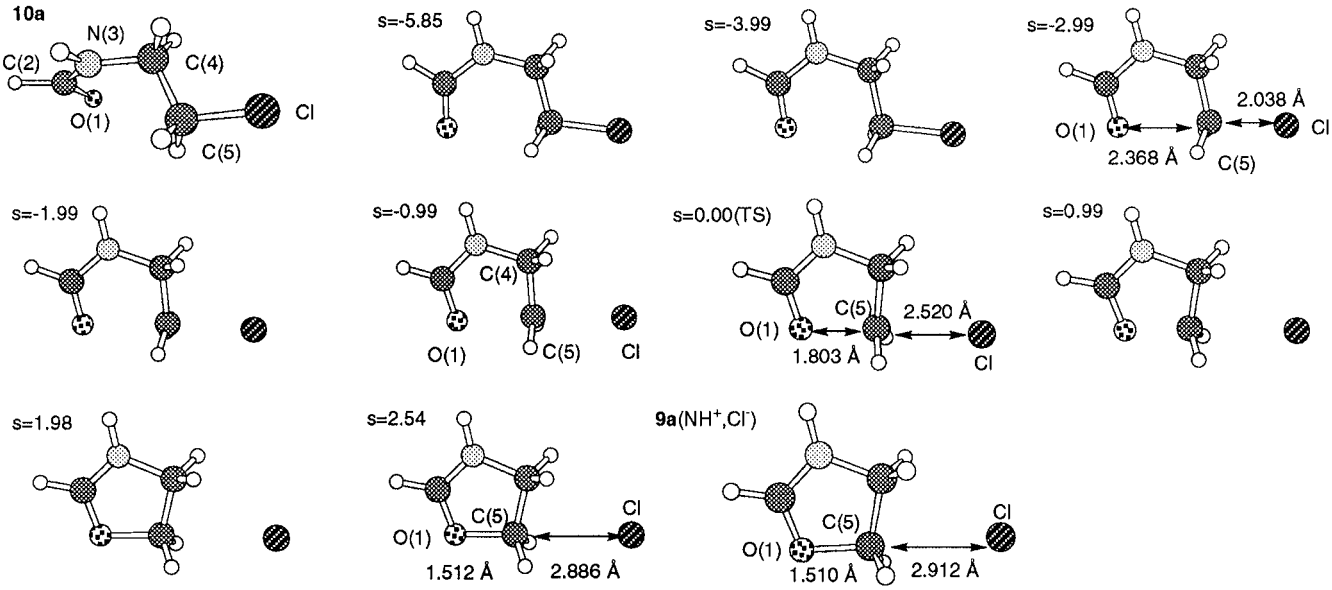

Figure 6. Geometry transformation along the IRC of the second S_N2 reaction from **10a** to **9a**(NH^+)+Cl^-. Values under the structures are the distances from the TS in $amu^{1/2}$ Bohr unit.[12]

in **8b**(5,NH^+,TS) than that in **8b**(4,NH^+,TS) because the N(3)−C(5) length in the former (2.253 Å) is longer by 0.096 Å than the N(3)−C(4) one in the latter (2.157 Å). It is, therefore, concluded that the reaction attacking at C(5) reaches the TS in the earlier stage than that at C(4).

The activation energies are estimated to be 28.2 and 39.8 kcal mol^{-1} for the mechanisms producing the 5-methyl product via **8b**(5,NH^+,TS) and the 4-methyl product via **8b**(4,NH^+,TS). A simple methyl substitution differentiates the activation energy for the S_Ni reaction by 11.6 kcal mol^{-1}. This energy difference is large enough to explain the experimental result that the only 5-methyl isomer was obtained for the reaction of **5** proceeding by the S_Ni mechanism. However, it must be pointed out that Cl^- and H^+ were adopted as a nucleophile and an acid, respectively, in the MO calculations while TsO^- and BF_3 were employed in the experiments.

Figure 7 also includes the transition state geometries obtained for the ring closure reaction which is the rate-determining step of the addition−elimination mechanism. While the O(1)−C(5) and C(5)−Cl lengths in **10b**(5,NH^+,TS) are 1.909 and 2.635 Å, the O(1)−C(4) and

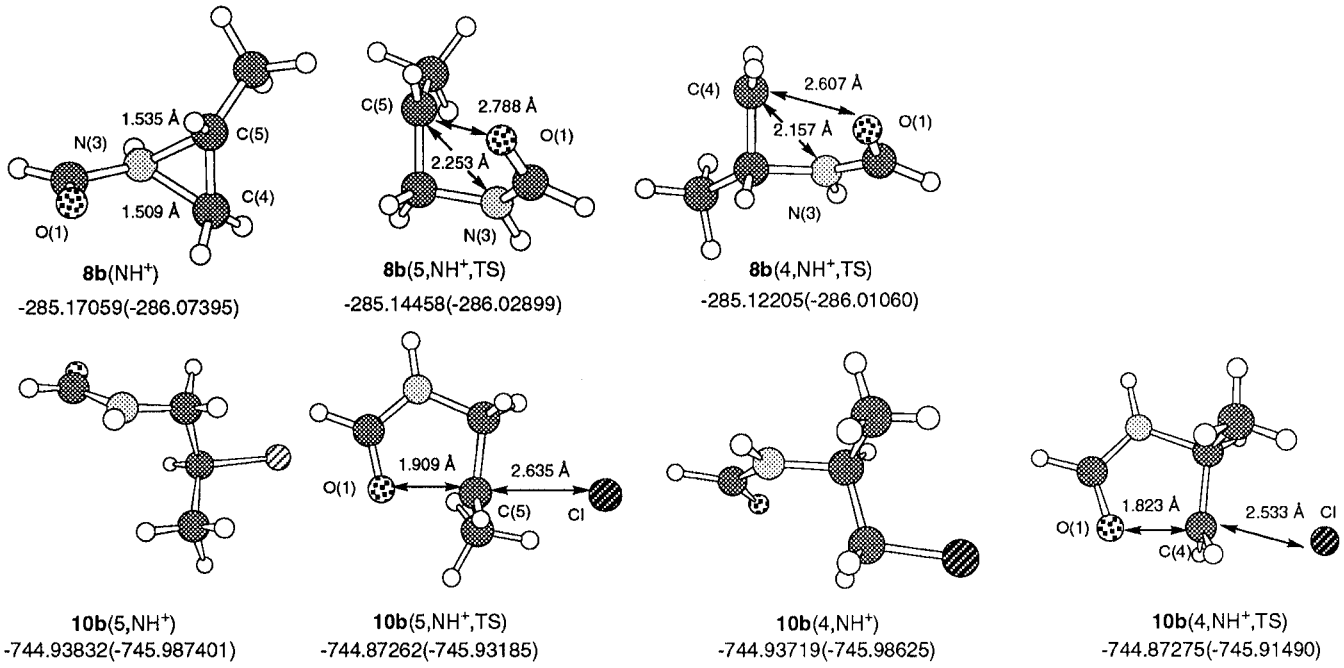

Figure 7. Optimized and TS structures for the methyl-substituted aziridines. Values under the molecules are the total energies in Hartree units calculated at the RHF/6-31G* (MP2/6-31G**//RHF/6-31G*) level of theory.

C(4)−Cl lengths in **10b**(4,NH^+,TS) are 1.823 and 2.533 Å, respectively. The former TS leads to the 5-methyl product and the latter TS to the 4-methyl product. Although the carbonyl oxygen O(1) as the nucleophile is located at a more distant position from O(1) in **10b**(5,NH^+, TS) than that in **10b**(4,NH^+,TS), the C−Cl bond in the former TS is weakened more in the latter TS. The activation energies are calculated to be 34.9 and 44.8 kcal mol^{-1}, respectively. These values are larger by more than 5−15 kcal mol^{-1} than those for the S_Ni mechanism. While the E_a to 4-methyl product is similar to the corresponding value for **10a** (45.4 kcal mol^{-1}), that to the 5-methyl product is smaller by 10.4 kcal mol^{-1} than that value.

Concluding Remarks

For the acid-catalyzed transformation of 1-acylaziridines to the oxazolines, we have shown both theoretically[17] and experimentally that there are two plausible mechanisms, which preserve the configuration of the carbons in the ring. The first is the path termed the S_Ni mechanism (the reaction catalyzed by H^+ or $BF_3{\cdot}OEt_2$), and the second is the addition−elimination involving the two S_N2 reactions (the double inversion concerned with Cl^- or TsO^-).

In the presence of the strong nucleophile Cl^-, the ring-opening reaction easily proceeds because of a small activation barrier of 14.0 kcal mol^{-1}. This value is smaller by 24.9 kcal mol^{-1} than that for the S_Ni mechanism. As the activation energy is as large as 45.4 kcal mol^{-1} for the subsequent ring closure reaction, the rate for the formation of the final product is expected to be very slow. However, a tosylate group in the ring-opened intermediate, which was used in the experiment, is apparently sufficiently better leaving group as compare to the chloride[18] so that the second S_N2 reaction proceeds on a reasonable time scale. The introduction of a methyl group at either C(4) or C(5) differentiate the activation barrier of this process.

In the absence of strong nucleophiles, the oxazoline formation proceeds by the S_Ni mechanism which has a smaller activation barrier than the second S_N2 reaction of the addition−elimination mechanism. While the methyl substituent at C(5) reduces the activation energy by more than 10 kcal mol^{-1}, that at C(4) increases that value by 0.9 kcal mol^{-1}. This is consistent with the exclusive formation of 5-methyl product in the reaction of **5**.

Experimental Section

General Information. Elemental analyses were performed by The Institute of Physical and Chemical Research, Wako, Saitama. (*S*)- or (*R*)-MTPA chloride was purchased from Aldrich Chemical Company (Milwaukee, WI). NMR spectra (^1H and ^{19}F) were recorded on a JEOL GSX-270 (270 MHZ for ^1H and 254 MHz for ^{19}F) spectrometer using $CDCl_3$ as a solvent, and TFA as a standard for ^{19}F NMR.

Preparation of (*R*)-[α-Methoxy-α-(trifluoromethyl)-phenylacetyl]-2(*S*)-methylaziridine (5). Into an ice-cooled solution of 63 mg (1.1 mmol) of (*S*)-2-methylaziridine and 110 mg (1.1 mmol) of Et_3N in ether was added a solution of 253 mg (1.0 mmol) of (*S*)-MTPA chloride in ether dropwise. After 2 h of stirring, the precipitated Et_3NHCl was removed by filtration, and the filtrate was washed with water, dried (Na_2SO_4), and concentrated on a rotary evaporator to give practically pure (*R*,*S*)-**5** in quantitative yield. Purification of **5** by column chromatography (*n*-hexane−ethyl acetate) gave analytical sample as an oil: ^1H NMR: δ 1.25 (d, 3H, J = 5.5,

(17) We have done the SCRF calculations of the IPCM method (ϵ = 2.0) at the MP2/6-31G**//RHF/6-31G* level of theory in order to estimate solvent effect, although we used the solvent in experiments with low a dielectric constant such as benzene. The activation energy for **8a**(NH^+) was estimated to be 38.8 kcal mol^{-1} which differs only by 0.1 kcal mol^{-1} from the value in the gas phase. The E_a of the double inversion mechanism were estimated to be 13.6 and 37.1 kcal mol^{-1} for the first and the second reactions, respectively. These values are differe by 0.4 and 8.3 kcal mol^{-1} from the gas phase value. Therefore, the potential profiles including solvent effect is not largely different from those without the solvent effect.

(18) March, J. *Advanced Organic Chemistry: Reactions, Mechanisms, and Structure*; 4th ed.; Wiley-Interscience: New York, 1992; p 357.

CCH_3), 1.99 (d, 1H, J = 3.7, Ha of 3-CH_2), 2.17 (d, 1H, J = 5.7, Hb of 3-CH_2), ~2.6 (m, 1H, 2-CH), 3.55 (d, 3H, J = 1.5, O-CH_3). ^{19}F NMR: δ 5.86. Anal. Calcd for $C_{13}H_{14}NO_2F_3$: C, 57.14; H, 5.16; N, 5.13. Found: C, 57.07, 56.97; H, 5.15, 5.14; N, 4.98, 5.14.

Compound (*S,S*)-**5** was prepared from (*S*)-2-methylaziridine and (*R*)-MTPA chloride in the same way as mentioned above. NMR spectral data of (*S,S*)-**5**: ^{1}H NMR: δ 1.20 (d, 3H, J = 5.5, C-CH_3), 1.91 (d, 1H, J = 3.7, Ha of 3-CH_2) 2.00 (d, 1H, J = 2.0, Hb of 3-CH_2), ~2.0 (m, 1H, 2CH), 3.71 (d, 3H, J = 1.8, O-CH_3). ^{19}F NMR: δ 6.05.

Reaction of 5 with BF_3·OEt_2. Into a refluxing solution of 80 mg (0.56 mmol) of BF_3·OEt_2 in benzene (dried over CaH_2, 0.5 mL) was added a solution of 0.5 mmol of (*R,S*)-**5** in benzene (0.5 mL) dropwise. After 15 min, the reaction mixture was cooled, washed with 2 N NaOH and brine, and then dried (Na_2SO_4). Evaporation of the solution on a rotary evaporator gave practically pure **6** as judged by ^{1}H and ^{19}F NMR in nearly quantitative yield. ^{19}F NMR analyses of the crude **6** showed that it was composed of 97% of (*R,S*) (δ 3.18) and 3 % of (*R,R*) (δ 3.21). Purification by column chromatography (benzene−ethyl acetate) gave analytical sample (oil): ^{1}H NMR: δ 1.32 (d, 3H, J = 6.2, CCH_3), 3.57 (d, 3H, J = 1.0, OCH_3), 3.65 (dd, 1H, J_{gem} = 14.7, J_{vic} = 7.3, Ha of 4-CH_2), 4.19 (dd, 1H, J_{gem} = 14.8, J_{vic} = 9.4, Hb of 4-CH_2), ~4.8 (m, 1H, 5-CH). Anal. Calcd for $C_{13}H_{14}NO_2F_3$: C, 57.14; H, 5.16; N, 5.13. Found: C, 57.37; H, 5.21; N, 5.09.

Reaction of (*S,S*)-**5** with BF_3·OEt_2 gave (*S,S*)-**6**: ^{1}H NMR: δ 1.40 (d, 3H, J = 6.2, C-CH_3), 3.35 (d, 3H, J = 1.3, OCH_3). ^{19}F NMR: δ 3.21.

Reaction of (*R,S*)-5 with *p*-Toluenesulfonic Acid. *p*-Toluenesulfonic acid monohydrate (102 mg, 0.54 mmol) was placed in a flask and heated at 110 °C under reduced pressure for 1 h to remove the water. Benzene (0.5 mL) was added to the flask, and the solution was heated to reflux. To the refluxing solution was added a solution of 0.5 mmol of (*R,S*)-**5** in benzene (0.5 mL), and the resulting solution was heated at reflux. After 15 min, about a half of the reaction mixture was removed, washed with 1 N NaOH followed by brine, and dried over anhydrous sodium sulfate. After evaporation of benzene on a rotary evaporator, the residue was submitted to NMR inspection. The ^{1}H NMR spectrum was practically the same as that of (*R,R*)-**7** except that it had a doublet at 1.34 (d, CCH_3 of (*R,S*)-**6**). By ^{19}F NMR analysis, it was found to be a mixture of (*R,R*)-**7** (δ 6.92, 92%) and (*R,S*)-**6** (δ 3.43,[19] 8%). After 1 h, the remaining reaction mixture was treated in the same manner. Inspection by ^{19}F NMR showed that the ratio of **7**/**6** was practically unchanged.

Preparation of Authentic Sample of (*R,R*)-7. From (*S*)-MTPA chloride and (*R*)-2-aminopropanol was obtained (*R*)-2-hydroxypropyl-(*R*)-MTPA amide (**7′**) as a syrup. Treatment of the crude **7′** with *p*-toluenesulfonyl chloride and pyridine gave (*R,R*)-**7** in crystalline form, which was recrystallized from benzene and *n*-hexane (50:50) to give analytical sample: mp 80−82 °C; ^{1}H NMR: δ 1.19 (d, 3H, J = 6.4, CCH_3), 2.45 (s, 3H, Ts-CH_3), 3.39 (d, J = 1.5, OCH_3), ~3.5 (m, 1H, Ha of CH_2), ~3.6 (m, 1H, Hb of CH_2), 4.74 (m, 1H, CH). ^{19}F NMR: δ 6.92. Anal. Calcd for $C_{20}H_{22}NO_5F_3S$: C, 53.92; H, 4.98; N, 3.15. Found: C, 54.27; H, 4.91; N, 3.07.

Preparation of Authentic Sample of (*R,S*)-6. To a solution of 150 mg of KOH in 3 mL of EtOH was added 150 mg of (*R,R*)-**7**, and the mixture was stirred at room temperature. As the spot of **7** disappeared on the TLC after 30 min, water was added to the mixture, and the mixture was concentrated on a rotary evaporator to remove EtOH. Benzene was added to the residue, and the organic layer was washed with brine, dried (Na_2SO_4), and concentrated to give 100 mg of crude (*R,S*)-**6**, which was purified by column chromatography using benzene and ethyl acetate. Both ^{1}H and ^{19}F NMR spectra coincided with those of isomerization product from (*R,S*)-**5** with BF_3·OEt_2.

Acknowledgment. The authors owe thanks to the Computer Center, Institute for Molecular Science at the Okazaki National Research Institutes, for the use of the NEC HSP computer and the Library Program GAUSSIAN92. This work is supported by the Grant-in-Aid for Scientific Research from the Ministry of Education of Japan.

Supporting Information Available: Z-matrices and energies of all structures (21 pages). This material is contained in libraries on microfiche, immediately follows this article in the microfilm version of the journal, and can be ordered from the ACS; see any current masthead page for ordering information.

JO961089N

(19) It was found that the ^{19}F NMR signal of CF_3 of **6** was shifted to lower field in the presence of **7**. Such a tendency was found to be pronounced when the ratio of **7**/**6** is large and the concentration of the solution is high.